

Analysis of Motion Errors of Linear Guide Pair Based on Parallel Mechanism [†]

Peng-Hao Hu ^{*}, Ying-Jun Lei [†] and Yang-Kai Ou

School of Instrument Science and Opto-Electronics Engineering, Hefei University of Technology, Hefei 230009, China; 2016170008@mail.hfut.edu.cn (Y.-J.L.); 2020010001@mail.hfut.edu.cn (Y.-K.O.)

* Correspondence: hupenghao@hfut.edu.cn; Tel.: +86-551-62901508

[†] This paper is an extended version of paper published in the Seventh International Symposium on Precision Mechanical Measurements (ISPMM7), Xia'men, China, 8–12 August 2015.

Abstract: This paper systematically summarized the technical state of art and research results on the motion error of a linear guideway, corrected some misconceptions, and further clarified the relationship between the straightness error of the guide rail itself and the motion error of the linear stage. Moreover, a new method based on parallel mechanism is provided to study the motion errors of the linear guide pair. The basic idea is to abstract the structural relationship between the stage and the guide rail into a 4-bar parallel mechanism. Thus, the stage can be considered as a moving platform in the parallel mechanism. Its motion error analysis is also transferred to moving platform position analysis in the parallel mechanism. The straightness motion error and angular motion error of the stage can be analyzed simultaneously by using the theory of parallel mechanism. Some experiments were conducted on the linear guideway of a self-developed parallel coordinate measuring machine. The experimental data and analysis verify the feasibility and correctness of this method.

Keywords: motion straightness error; angular motion error; parallel mechanism



Citation: Hu, P.-H.; Lei, Y.-J.; Ou, Y.-K. Analysis of Motion Errors of Linear Guide Pair Based on Parallel Mechanism. *Machines* **2021**, *9*, 33. <https://doi.org/10.3390/machines9020033>

Academic Editor: Dan Zhang
Received: 12 January 2021
Accepted: 3 February 2021
Published: 5 February 2021

Publisher's Note: MDPI stays neutral with regard to jurisdictional claims in published maps and institutional affiliations.



Copyright: © 2021 by the authors. Licensee MDPI, Basel, Switzerland. This article is an open access article distributed under the terms and conditions of the Creative Commons Attribution (CC BY) license (<https://creativecommons.org/licenses/by/4.0/>).

1. Introduction

The linear guide pair is widely used in machine tools, precision instruments, and other precision equipment. A normal serial type three-axis NC machine tool is constructed in three linear stages to provide motions in the X, Y, and Z directions. The traditional coordinate measuring machine is built with similar structures. However, each axis contains several geometric errors caused by manufacturing errors of the parts and assembly errors of the stages. Combining this with the problem of motion errors of guideways encountered in our development of a parallel coordinate measuring machine, we intend to elaborate and share knowledge and understanding about this issue with our predecessors and colleagues.

1.1. Cognition about Motion Errors of Linear Guide Pair

The linear motion stage suffers from various errors, such as manufacturing error, assembly error, and errors induced by force. Therefore, 5-DOF additional and unexpected error motion will appear on the stage, as shown in Figure 1. According to ISO 230-1:2012 [1], such geometric errors include three angular motion errors (E_{CX} , E_{BX} , and E_{AX}) and two straightness motion errors, E_{YX} and E_{ZX} . However, in many Chinese studies, these errors are translated into “guide motion error”. The expression is not accurate; although it is related to the straightness manufacturing error of the rail itself, the guide rail itself is static, and this error is generated on the stage during its movement. Therefore, this error should be referred to as the motion error of the guide pair in Chinese studies [2,3].

The straightness motion error of the stage is closely related to the straightness error of the guide rail itself. Therefore, some confusion arises between these two concepts. The straightness error of the guide rail itself is a form error, which needs to be calculated and evaluated after measurement. It has a definite shape of tolerance zone, whereas the

straightness motion error reflects the deviation of the stage from the ideal axis in its motion, which is not a form error and does not need to be evaluated. To obtain this deviation, we study many measurement methods and error separation techniques to improve the accuracy of machine tools or instruments by error compensation.

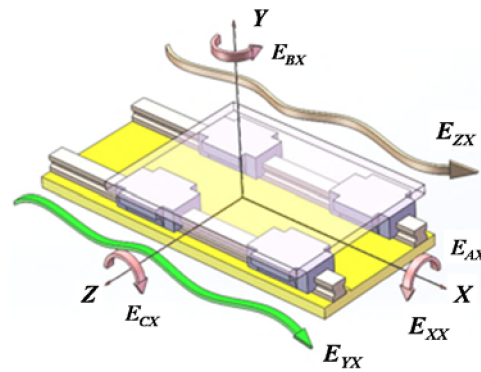


Figure 1. 6-DOF geometric errors of a linear moving stage.

The straightness motion error of the linear stage is closely related to the straightness error of the guide rail itself, but these errors are different in that the guide rail straightness error is a cause, whereas the straightness motion error is an effect. Furthermore, the assembly errors, the stiffness of the base, the deformation, and the load on the stage also influenced the effect. This issue has attracted the attention of many scholars around the world, who have conducted extensive research and achieved many valuable results [4–7].

1.2. Summary of the Relationship between Slider Motion Error and Angular Motion Error

We study angular motion error because this type of error will produce an Abbe error and transmit it to the instrument or machine tool. Angular motion error is the root of the Abbe error. The Abbe principle was published in 1890. It gives us the design idea and principle needed to superficially improve the accuracy of the instrument. In essence, the influence of the angular motion error of the stage on the measurement results is eliminated through structural design [8]. In 1979, Bryan updated the Abbe principle conception. He qualitatively expanded the relationship between the slider motion error, the angular motion error, and the straightness error of the guide rail itself. A more important contribution is that the Abbe principle was extended to the straightness motion error of the linear stage [9]. In other words, when we deal with or analyze the error of an instrument or machine tool, the straightness motion error corresponds to Bryan's proposal, while the angular motion error corresponds to the traditional Abbe principle [10].

In many articles, the straightness motion error of the stage is expressed as the integration of angular motion error, or the rotational errors can be obtained reversely by differentiating straightness errors [11–13]. A high correlation seems to be emphasized between the straightness motion error and the angular motion error. Conversely, some researchers treat them as mutually independent [14,15]. Ekinci depicted the relationship among straightness motion error, angular motion error, and geometric error of the guider itself, as shown in Figure 2. In this concept, only one guider rail exists, and the carriage is supported by two linear blocks, which are abstracted as two small wheels separated by distance L . The carriage moves on a guide rail with a geometric $\Delta z(x)$. Therefore, the straightness motion error $\delta_z(x)$ in the Z direction and the angular pitch error $\alpha(x)$ can be described as

$$\begin{cases} \alpha(x) = \frac{\Delta(x+\frac{L}{2}) - \Delta(x-\frac{L}{2})}{L} \\ \delta_z(x) = \frac{\Delta(x+\frac{L}{2}) + \Delta(x-\frac{L}{2})}{2} \end{cases} \quad (1)$$

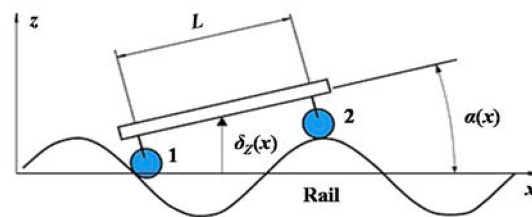


Figure 2. Stage-rails configuration.

Ekinci also provided a detailed analysis of this viewpoint. The accuracy of the calculation of the straightness deviation integrals from the rotation deviation depends on the ratio between the length of the guide and the wavelength deviation in the rail [13]. Majda presented a new approach to modeling geometric errors of linear guideways for machine tools. This approach was applied by interpreting the results of experimental examinations of angular kinematic errors obtained for a real machine tool. The paper originally aimed to verify the usefulness of the concept of calculating kinematic straightness errors from angular errors, but the conclusion is that no close relationship was found between the two types of error. Moreover, straightness and angular errors on machine tools or instruments should be treated as independent of each other [16].

In general, a great straightness error of the rail corresponds to a great straightness motion error and angular motion error of the stage. However, no direct functional relationship exists between them. When we measure and evaluate the straightness error of the guide rail by using an autocollimator or spirit level, we measure the angle error first and then convert it into displacement to construct the straightness error curve. The data processing involves accumulation and integration. This approach is the measurement method and mathematical means for evaluating the straightness error of the guide rail itself. This idea does not mean that a similar mathematical causality relationship exists between the straightness motion error and the angular motion error of the stage.

2. New Idea about Analysis of Linear Motion Error

Generally, the motion error analysis of stage is based on rigid body motion and pure geometry without considering the elasticity, stress, and deformation of involved parts in their motion. Thus, the analysis is not conducted according to the actual assembly and working conditions of the stage. If the straightness error of the guide rail itself or the manufacturing error of the related parts is large, then the intuitive phenomenon is that the stage will not move smoothly, or is even stuck, because of the increase in friction and motion resistance. When increasing the magnitude of interference between the components or generating additional elastic deformations in the relevant parts to tolerate this error, all these behaviors maintain the stage action. However, they increase friction and bring about inevitable slider motion errors. On the basis of force and moment equilibrium, and considering the deformation of the involved parts, many scholars have conducted research on the straightness error motion of the linear stage. Representative achievements are as follows.

Majda presented a new approach to modeling the geometric errors of linear guideways for machine tools, taking into consideration the strains of the table due to guideway geometric errors. This approach was used to interpret the results of experimental examinations of angular kinematic errors obtained for a real machine tool [17]. Ohta et al. presented a flexible model that considers the flexibility of the table and rail. The calculated vertical stiffness of linear bearing using this model more closely matches the measured stiffness [18].

The easiest way to analyze the 5-DOF motion errors is to apply finite element analysis to the entire stage under equilibrium conditions for the forces and moments. However, the model becomes cumbersome and complex for 5-DOF and is difficult to apply to various types of stages. Korean scholars also made contributions to this issue. They proposed

a transfer function method to describe the characteristics of the linear motion bearing, which represents the bearing force variation of a bearing block with respect to the spatial frequency components of the rail form error. The transfer function can be used positively to predict the motion error of a table with multiple bearing blocks, in which the bearing forces are derived from the rail form error by using the transfer function [19,20]. The algorithm can also be used reversely to estimate the rail form error after assembly on the reference surface from the measured linear and angular motion errors [21]. Fan et al. proposed a kinematic errors prediction method for the machine tool's guideways based on tolerance by formulating the relationship between tolerance and geometric profile errors of guideways on the machine tools. This method is convenient for engineers to derive the distribution of kinematic errors in their design [22]

The issue now is if we can consider the actual situation and use new ideas or theories to analyze and discuss the motion errors of the stage. During the research and development of parallel coordinate measuring machines, we found that many parallel mechanisms only have numerical solutions and cannot obtain analytical solutions. The essence of numerical solutions is to keep approaching, iterating, and then achieving convergence. In real parallel mechanism motion, the position of the moving platform is determined by the plurality of bars in common. In this process, mechanical tensile, compression, torsion, and elastic deformation of involved parts occur. When a certain position can achieve a balance among these factors, then this position is the actual position that the moving platform reaches. This process is mathematically reflected by iteration and convergence. A similar process exists in the actual motion of rail pairs [23,24].

In addition, due to 5-DOF additional and unexpected error motions of the stage on the linear guide pair, the corresponding angular motion errors and straightness motion errors are generated, as shown in Figure 1. In the motion of the parallel mechanism, the moving platform also moves, with multi-DOF. The multi-DOF of real motions between them is similar. According to the linear guide pairs, the stage rides on two rails by four linear blocks. Its error motion is influenced and determined by the four linear blocks. In parallel mechanism, the position of the moving platform is also determined by the multiple branch chains, which is similar to the stage with four linear blocks.

Therefore, we attempt to abstract the structure relation of the stage and rail as a four-bar parallel mechanism. Then, the stage can be considered as a moving platform in the parallel mechanism. Its motion error analysis is also transferred to moving platform position analysis in the parallel mechanism.

3. Modeling of Stage Motion Error

For convenience of analysis, only the straightness error of the rail itself in the Z direction will be discussed without consideration of its straightness error in the Y direction, as Figure 3a shows. The stage rides on two rails by four linear blocks. Here, the matched pairs of blocks and rail can be simplified as a 2-RPS-2-SPS parallel mechanism, as shown in Figure 3b. The RPS branched chain consists of a revolute pair, prismatic pair and spherical joint. The SPS branched chain consists of a spherical joint, prismatic pair and spherical joint. The linear deviation of the rail in the Z direction is considered as the variation in rod length in the parallel mechanism.

According to the modified Kutzbach–Grubler formula of degree of freedom, the degree of freedom of the 2-RPS-2-SPS parallel mechanism can be obtained

$$M = 6(n - g - 1) + \sum_{i=1}^g f_i - \varepsilon = 6(10 - 12 - 1) + 24 - 2 = 4 \quad (2)$$

where M is the degree of freedom of the mechanism, n is the total number of components, g is the number of motion pairs, f_i is the degree of freedom of the i -th motion pair. There is a local degree of freedom of rotating around its axis between the two ball hinges at the SPS branch chain, and local degree of freedom $\varepsilon = 2$. The 2-RPS branch chains and 2-SPS branch chains are set along the X-axis, respectively, presenting a partial symmetrical structure that

means parallel mechanism has four degrees of freedom including $\alpha(x)$ rotation around the Y-axis, $\beta(x)$ around the X-axis (we usually refer to them as pitch and roll), and the $\delta_z(x)$ and $\delta_x(x)$ movements along the Z and X-axes shown in Figure 3b.

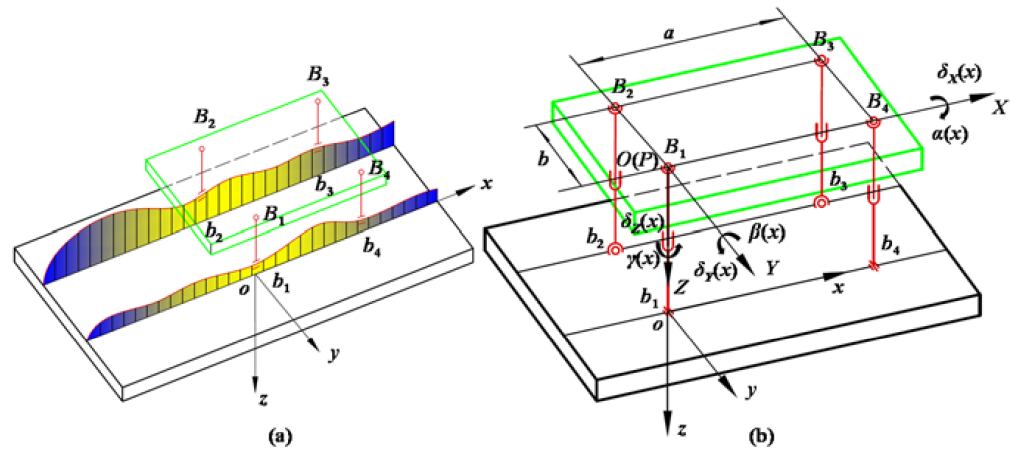


Figure 3. (a) Moving error model of guideway, (b) simplified parallel mechanism model.

From the perspective of parallel mechanism, the base plane where the two rails sit is the static platform. The stage can be taken as a moving platform. They are connected by two RPS branch chains and two SPS branch chains. The linear deviation of the rail in the Z direction is considered as the variation in the length of branch chains in the 2-RPS-2-SPS parallel mechanism, L_1-L_4 are the length of the branch chain shown in Figure 3b [25].

Taking the joint center point B_1 on the moving platform as the coordinate origin, the moving coordinate system O-XYZ is established and the XOY plane is parallel to the installation plane of the two guide rails. The static coordinate system o-xoy is established by taking the joint center point b_1 in each pose as the coordinate origin. The xoy plane is also parallel to the installation plane of the two guide rails.

$b_i = (b_{xi}, b_{yi}, b_{zi})^T$ is the coordinate vector of the joint center point in the static coordinate system o-xyz; $B_i = (B_{Xi}, B_{Yi}, B_{Zi})^T$ represents the coordinate vector of each joint center point at the moving platform in the moving coordinate system O-XYZ, and $X = (x_p, y_p, z_p)^T$ is the coordinate vector of the origin point of the moving coordinate system in the static coordinate system. The coordinates of every joint center points are shown in Table 1, $i = 1, 2, 3, 4$. $a = 140$ mm, $b = 100$ mm in the self-developed parallel coordinate measuring machine.

Table 1. Position of joint.

Branch i	Centers of Joint b_i			Centers of Joint B_i		
	b_{xi}	b_{yi}	b_{zi}	B_{Xi}	B_{Yi}	B_{Zi}
1	0	0	0	0	0	0
2	0	$-b$	0	0	$-b$	0
3	a	$-b$	0	a	$-b$	0
4	a	0	0	a	0	0

Since this parallel mechanism did not consider the rotation around the Z-axis, the pose transformation matrix R can be simplified as

$$R = \begin{bmatrix} \cos \beta(x) & \sin \alpha(x) \sin \beta(x) & \cos \alpha(x) \sin \beta(x) \\ 0 & \cos \alpha(x) & -\sin \alpha(x) \\ -\sin \beta(x) & \sin \alpha(x) \cos \beta(x) & \cos \alpha(x) \cos \beta(x) \end{bmatrix} \quad (3)$$

Therefore, by coordinate transformation, the vector B_i on the moving platform is transformed into the static coordinate system o-xyz, which can be expressed as C_i

$$C_i = RB_i + X \quad (4)$$

Length vector L_i can be expressed as

$$L_i = RB_i + X - b_i \quad (5)$$

where $L_i = (l_{ix}, l_{iy}, l_{iz})^T$, and the length of the top and lower joint of branched chain L_i is

$$L_i = |L_i| = \sqrt{l_{ix}^2 + l_{iy}^2 + l_{iz}^2} \quad (6)$$

Since this parallel mechanism did not consider the translational motion in the the Y-axis, $y_p = 0$, substituting the coordinate values of each joint into Equation (6), the following formula can be obtained

$$\begin{cases} L_1^2 = (x_p)^2 + (z_p)^2 \\ L_2^2 = [x_p - b \sin \alpha(x) \sin \beta(x)]^2 + [-b \cos \alpha(x) + b]^2 \\ \quad + [z_p - b \sin \alpha(x) \cos \beta(x)]^2 \\ L_3^2 = [x_p + a \cos \beta(x) - b \sin \alpha(x) \sin \beta(x) - a]^2 + [-b \cos \alpha(x) + b]^2 \\ \quad + [z_p - a \sin \beta(x) - b \sin \alpha(x) \cos \beta(x)]^2 \\ L_4^2 = [x_p + a \cos \beta(x) - a]^2 + [z_p - a \sin \beta(x)]^2 \end{cases} \quad (7)$$

After the parallel mechanism structure parameters are identified, the length of the branch chain contains all the information about the pose and position. Thus, on the basis of the length change in the rod, the original position is selected to obtain the inverse motion position variables. Then, the length of rod numerical in different pose and position are integrated into the forward solution model of the parallel mechanism, and the fsolve function in MATLAB is used to iterate the nonlinear function groups to gradually approach the real length of the rod. First, the original position of the moving platform is assumed as $(x_{p0}, z_{p0}, \alpha_0, \beta_0)$. Through the analysis of inverse kinematics position, the posture of rod length L_i^1 is obtained. The length of the rod is as L_i , and the difference between L_i^1 and L_i is $\Delta L_i^1 = L_i - L_i^1$. L_i is the position variable function $(x_p, z_p, \alpha, \beta)$ of the moving platform. It can be obtained as

$$\begin{bmatrix} \Delta L_1^{(1)} \\ \Delta L_2^{(1)} \\ \Delta L_3^{(1)} \\ \Delta L_4^{(1)} \end{bmatrix} \times \begin{bmatrix} \frac{\partial L_1}{\partial x} & \frac{\partial L_1}{\partial z} & \frac{\partial L_1}{\partial \alpha} & \frac{\partial L_1}{\partial \beta} \\ \frac{\partial L_2}{\partial x} & \frac{\partial L_2}{\partial z} & \frac{\partial L_2}{\partial \alpha} & \frac{\partial L_2}{\partial \beta} \\ \frac{\partial L_3}{\partial x} & \frac{\partial L_3}{\partial z} & \frac{\partial L_3}{\partial \alpha} & \frac{\partial L_3}{\partial \beta} \\ \frac{\partial L_4}{\partial x} & \frac{\partial L_4}{\partial z} & \frac{\partial L_4}{\partial \alpha} & \frac{\partial L_4}{\partial \beta} \end{bmatrix} = \begin{bmatrix} \Delta x_p^{(1)} \\ \Delta z_p^{(1)} \\ \Delta \alpha^{(1)} \\ \Delta \beta^{(1)} \end{bmatrix} \quad (8)$$

where $\Delta L_i^{(1)}$ is the first-time length-modified increment, and $(\Delta x_p^{(1)}, \Delta z_p^{(1)}, \Delta \alpha^{(1)}, \Delta \beta^{(1)})^T$ is the position-fixed increment for the first time. The first fixed position of the moving platform can be rewritten as

$$\begin{aligned} & (x_{p1}, z_{p1}, \alpha_1, \beta_1)^T \\ & = (x_{p0} + \Delta x_p^{(1)}, z_{p0} + \Delta z_p^{(1)}, \alpha + \Delta \alpha^{(1)}, \beta + \Delta \beta^{(1)})^T \end{aligned} \quad (9)$$

Then, the first-time fixed position of the moving platform is taken as the initial value to iterate again, with the process repeated n times until the expected accuracy is reached. The position $(x_{pn}, z_{pn}, \alpha_n, \beta_n)^T$, at this point, is the actual position under the length of rod L_i and is also the expected result.

4. Experiment and Data Analysis

Figure 4 shows the straightness of two long rails (2000 mm) in the Z direction is measured on a self-developed 3-PUU parallel CMM by using the traditional autocollimator. The experiment was carried out at a temperature of 20 ± 1 °C. The autocollimator (model: JJ-99 from Jingda Measurement Technology Co. Ltd. Jiujiang, China) is used. The measuring range is ± 10 s and the resolution is 0.1 s. The straightness error curves of the two rails after the original data processing are shown in Figure 5 [26].

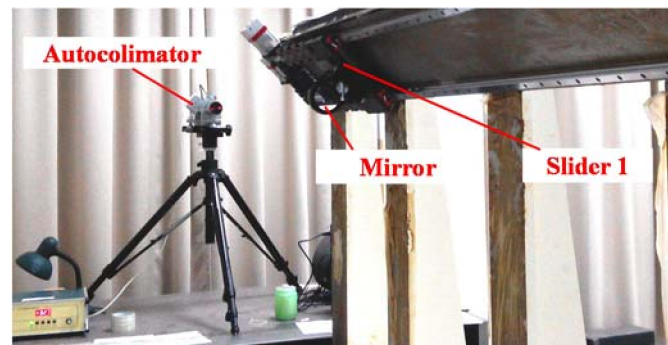


Figure 4. Measurement of straightness of two rails.

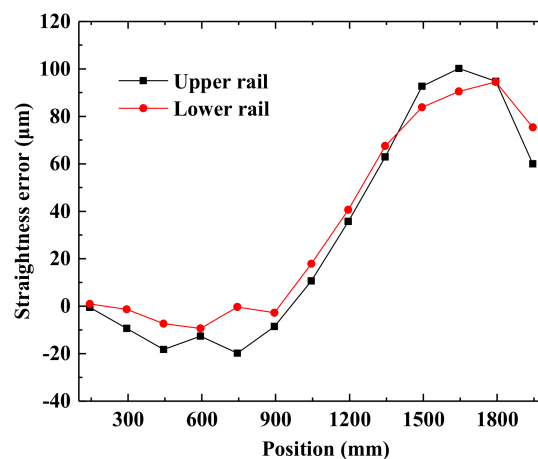


Figure 5. Straightness error in Z direction of two rails.

In accordance with the above straightness error of two rails in Figure 5, the least square method is used to fit the straightness deviation equation for the two rails in the Z direction along the X-axis [26]

$$\begin{cases} z_1 = -1.349 \times 10^{-13}x^4 + 4.192 \times 10^{-10}x^3 \\ \quad -2.975 \times 10^{-7}x^2 + 0.015 \times 10^{-3}x + 2.352 \times 10^{-3} \\ z_2 = -9.965 \times 10^{-14}x^4 + 3.216 \times 10^{-10}x^3 \\ \quad -2.495 \times 10^{-7}x^2 + 0.041 \times 10^{-3}x - 0.711 \times 10^{-3} \end{cases} \quad (10)$$

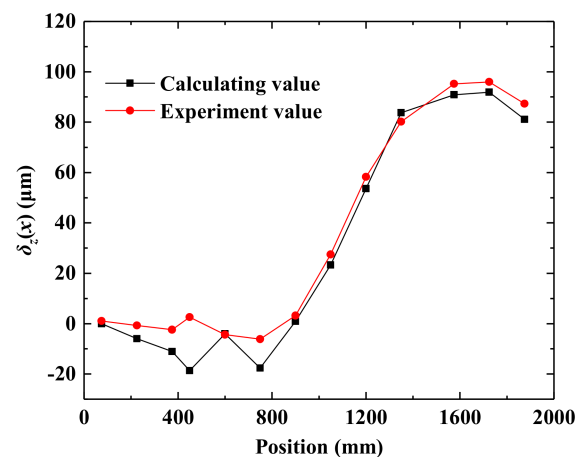
Thirteen center positions of the stage are selected for simulation calculation with 150 mm spacing, $x = 75, 225, 375, 450, \dots, 525, \dots, 1875$. With the use of Equation (8), values of straightness on four points b_1, b_2, b_3, b_4 can be obtained, taking them as the variation in rod length into the above model of the parallel mechanism. The iteration results obtained by using the fsolve function in MATLAB are shown in Table 2 [26].

Table 2. Stage position and orientation.

No.	X_0 (mm)	ΔX (μm)	$\delta_z(x)$ (μm)	Pitch $\beta(x)$ (")	Roll $\alpha(x)$ (")
1	75	0.24	0	1.83	2.52
2	225	-3.88	-6.00	-4.32	2.84
3	375	-3.02	-11.11	-9.39	2.06
4	450	2.16	-18.66	2.86	0.00
5	600	4.00	-4.01	-17.79	1.54
6	750	-1.93	-17.58	3.51	0.01
7	900	-8.75	0.91	7.15	-1.75
8	1050	-16.56	23.32	11.49	-1.32
9	1200	-26.78	53.65	11.38	-0.58
10	1350	-14.10	83.77	13.27	0.11
11	1575	-19.34	90.87	5.38	3.90
12	1725	-0.98	91.88	-9.61	2.13
13	1875	1.30	81.11	-10.40	2.79

In the third column of Table 2, the value of ΔX is the additional motion error in the X direction caused by the straightness error of the guide rail. This result is different from E_{XX} Figure 1, which is generally called the positioning error along the moving axis. Generally, we always consider that the positioning error is mainly determined by the driving system and controlling system. Here, we found that the straightness error of rails will also provide an additional motion error to the X-axis and contribute to the total position error $\delta_x(x)$.

The fourth column in Table 2 shows the calculation result of $\delta_z(x)$; its variation curve is shown by the red line in Figure 6. The black curve in Figure 6 is the straightness motion error of the center on the stage in the Z direction, measured directly by the laser interferometer (model: XL80 from Renishaw Co. Ltd. London, UK); the experiment was carried out at the temperature of 20 ± 1 °C [27]. By comparing the two curves, we can see that the two curves basically coincide, which means the above analysis is a feasible method.

**Figure 6.** Results comparison of $\delta_z(x)$.

We also compare the calculated pitch angle in the fifth column with the actual pitch error measured by the autocollimator. The comparison results are shown in Figure 7, and their variation tendency is similar. The data of the roll angle were not compared because measuring the roll angle by using the autocollimator is inconvenient. We will continue this work in the near future.

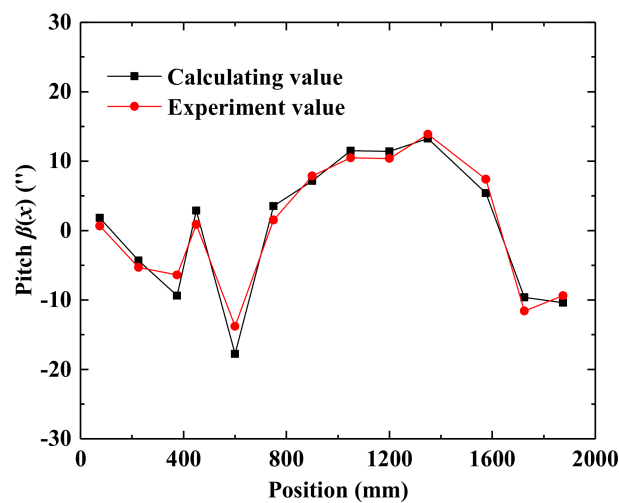


Figure 7. Results comparison of pitch $\beta(x)$.

5. Conclusions

This paper analyzes the causal relationship between the straightness error of the guide rail and the motion error of the stage. It also clarifies the correlation between the straightness motion error and the angular motion error. On the basis of the theory of parallel mechanism, a method for simultaneous analysis of straightness and angular motion errors in stage is presented. The core of this method is to transform the problem of stage motion error into finding the correct solution of the parallel mechanism with a variable rod length. The corresponding theoretical calculation model is established. The comparison between theoretical calculation results and experimental data proves the validity of this method, thereby providing a new method for analyzing the motion error of guideway pairs.

Author Contributions: The authors' contributions are as follows: P.-H.H. provided thoughts and wrote the manuscript; Y.-J.L. and Y.-K.O. finished experiment, sampling and data analysis; Y.-J.L. edited the manuscript. All authors have read and agreed to the published version of the manuscript.

Funding: This research was funded by the National Natural Science Foundation of China, grant number 51475133 and 51675157.

Institutional Review Board Statement: Not applicable.

Informed Consent Statement: Not applicable.

Data Availability Statement: Not applicable.

Conflicts of Interest: The authors declare no conflict of interest.

References

- ISO 230–1: 2012. *Test Code for Machine Tools—Part 1: Geometric Accuracy of Machines Operating Under No-Load or Quasi-Static Conditions*; International Organization for Standardization: Geneva, Switzerland, 2012.
- Yang, J.; Feng, Q. Research progress on volumetric geometric error measurement of numerical control (NC) machine tools. *Chin. J. Sci. Instrum.* **2017**, *38*, 1901–1911. (In Chinese)
- Wu, Y.; Shen, H.; Sun, X.; Wang, D. 5D error prediction model for elastic prismatic pair of machine tool. *J. Huahong Univ. Sci. Technol. Nat. Sci. Ed.* **2019**, *47*, 121–126. (In Chinese)
- Tong, V.; Kwon, S.; Hong, S. Modeling of moving table with linear roller guides subjected to geometric errors in guide rails. *Int. J. Precis. Eng. Manuf.* **2020**, *21*, 1903–1919. [[CrossRef](#)]
- Schwenke, H.; Knapp, W.; Haitjema, H.; Weckenmann, A.; Schmitte, R.; Delbressine, F. Geometric error measurement and compensation of machines—An update. *Cirp Ann.* **2008**, *57*, 660–675. [[CrossRef](#)]
- Ni, Y.; Zhou, H.; Shao, C.; Li, J. Research on the error averaging effect in a rolling guide pair. *Chin. J. Mech. Eng.* **2019**, *32*, 72. [[CrossRef](#)]
- Rahmani, M.; Bleicher, F. Experimental and numerical studies of the influence of geometric deviations in the performance of machine tools linear guides. *Procedia CIRP* **2016**, *41*, 818–823. [[CrossRef](#)]

8. Abbe, E. Messapparate für physiker. *Z. Instrum.* **1890**, *10*, 446–448.
9. Bryan, J. The Abbe principle revisited: An updated interpretation. *Precis. Eng.* **1979**, *1*, 129–132. [[CrossRef](#)]
10. Huang, Y.; Fan, K.; Lou, Z.; Sun, W. A novel modeling of volumetric errors of three-axis machine tools based on Abbe and Bryan principles. *Int. J. Mach. Tools Manuf.* **2020**, *151*, 103527. [[CrossRef](#)]
11. Biral, F.; Bosetti, P. On-line measurement and compensation of geometrical errors for Cartesian numerical control machines. In Proceedings of the 9th IEEE International Workshop on Advanced Motion Control, Istanbul, Turkey, 27–29 March 2006; pp. 120–125.
12. Srivastava, A.; Veldhuis, S.C.; Elbestawit, M.A. Modelling geometric and thermal errors in a five-axis CNC machine tool. *Int. J. Mach. Tools Manuf.* **1995**, *35*, 1321–1337. [[CrossRef](#)]
13. Ekinici, T.; Mayer, J. Relationships between straightness and angular kinematic errors in machines. *Int. J. Mach. Tools Manuf.* **2007**, *47*, 1997–2004. [[CrossRef](#)]
14. Ahn, K.; Min, B.; Pasek, Z. Modeling and compensation of geometric errors in simultaneous cutting using a multi-spindle machine tool. *Int. J. Adv. Manuf. Technol.* **2006**, *29*, 929–939. [[CrossRef](#)]
15. Okafor, A.; Ertekin, Y. Vertical machining center accuracy characterization using laser interferometer: Part 1. Linear positional errors. *J. Mater. Process. Technol.* **2000**, *105*, 394–406. [[CrossRef](#)]
16. Majda, P. Relation between kinematic straightness errors and angular errors of machine tool. *Adv. Manuf. Sci. Technol.* **2012**, *36*. [[CrossRef](#)]
17. Majda, P. Modeling of geometric errors of linear guideway and their influence on joint kinematic error in machine tools. *Precis. Eng.* **2012**, *36*, 369–378. [[CrossRef](#)]
18. Ohta, H.; Tanaka, K. Vertical stiffnesses of preloaded linear guideway type ball bearings incorporating the flexibility of the carriage and rail. *J. Tribol.* **2010**, *132*, 011102. [[CrossRef](#)]
19. Khim, G.; Oh, J.; Park, C. Analysis of 5-DOF motion errors influenced by the guide rails of an aerostatic linear motion stage. *Int. J. Precis. Eng. Manuf.* **2014**, *15*, 283–290. [[CrossRef](#)]
20. Hwang, J.; Park, C.; Kim, S. Estimation method for errors of an aerostatic planar XY stage based on measured profiles errors. *Int. J. Adv. Manuf. Technol.* **2010**, *46*, 877–883. [[CrossRef](#)]
21. Khim, G.; Park, C.; Shamoto, E.; WooKim, S. Prediction and compensation of motion accuracy in a linear motion bearing table. *Precis. Eng.* **2011**, *35*, 393–399. [[CrossRef](#)]
22. Fan, J.; Tao, H.; Wu, C.; Li, Z. Kinematic errors prediction for multi-axis machine tools' guideways based on tolerance. *Int. J. Adv. Manuf. Technol.* **2018**, *98*, 1131–1144. [[CrossRef](#)]
23. Hu, P.; Zhang, J.; Ma, X.; Fei, Y. Analysis of Slider Motion Error on 3-PUU Parallel Coordinate Measuring Machine. *J. Mech. Eng.* **2015**, *51*, 45–50. (In Chinese) [[CrossRef](#)]
24. Hu, P.; Yu, C.; Fan, K.; Dang, X.; Li, R. Error averaging effect in parallel mechanism coordinate measuring machine. *Appl. Sci.* **2016**, *6*, 383. [[CrossRef](#)]
25. Huang, Z.; Li, Q.; Ding, H. *Theory of Parallel Mechanisms*; Springer: Dordrecht, The Netherlands, 2013.
26. Ma, X. *Slider Motion Error Influence on 3-PUU Parallel Coordinate Measuring Machine*; Hefei University of Technology: Hefei, China, 2016. (In Chinese)
27. Zhang, J. *A Study on 3-PUU Parallel Coordinate Measuring Machine Error*; Hefei University of Technology: Hefei, China, 2015. (In Chinese)